Catalysis Letters
https://doi.org/10.1007/s10562-021-03728-z

SBA-15 Supported Dendritic ILs as a Green Catalysts for Synthesis of 2-Imidazolidinone from Ethylenediamine and Carbon Dioxide

Qingwang Min[1] · Penghua Miao[1] · Jinghan Liu[1] · Jianjun Ma[1] · Meijuan Qi[1] · Farzaneh Shamsa[2]

Received: 6 March 2021 / Accepted: 3 July 2021

Abstract

In this work, a simple and facile approach is conducted for preparing many new SBA-15 supported dendritic imidazolium ILs heterogeneous catalysts SBA-15/IL(1–3) having high ionic density from SBA-15. SBA-15/IL(3) as a green heterogeneous catalyst can be used for synthesis of 2-imidazolidinone from ethylenediamine and carbon dioxide and considering solvent-free condition. SBA-15/IL(3) showed to have the highest catalytic activity besides a positive dendritic influence on the yields of the synthesis of 2-imidazolidinone in the presence of CO_2 is seen because of existing the high-density peripheral zwitterionic ionic liquid functional groups on the biobased SBA-15/IL(3) catalyst surfaces.

Graphical Abstract

SBA-15 supported dendritic ILs as a green catalysts for synthesis of 2-imidazolidinone from ethylenediamine and carbon dioxide

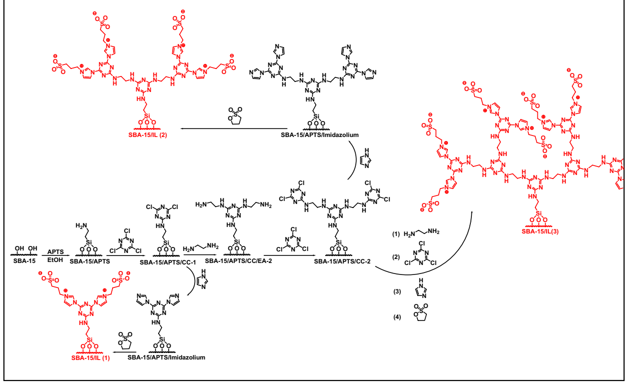

Keywords Nanocatalyst · Green chemistry · SBA-15 · Ionic liquid · 2-imidazolidinone · CO_2

1 Introduction

Usually, many diamines reactions having many types of reagents utilized as carbonyl sources like carbonyl selenide [1], phosgene, urea, organic carbonates [2, 3], dithiocarbonate [4] and carbonyldiimidazole [5]. The reaction process of CO_2 with a diamine is a direct eco-friendly procedure in the synthesis of cyclic urea from the toxic point of mentioned reagents. In the term of this reaction, scholars demonstrated homogeneous catalysts like $TBA_2[WO_4]$ [6] and Ph_3SbO/

✉ Qingwang Min
minqw@dlpu.edu.cn

✉ Farzaneh Shamsa
Farzaneh.Shamsa@gmail.com

[1] School of Light Industry and Chemical Engineering, Dalian Polytechnic University, Dalian 116034, PR China

[2] Young Researchers and Elite Club, Neyshabur Branch, Islamic Azad University, Neyshabur, Iran

P_4S_{10} [7] as efficient catalysts together with many limitations such as recyclability, catalyst separation, and high cost of catalyst production. In the Refs. [8] and [9], scholars have suggested non-catalytic approaches to synthesis cyclic urea, directly, from diamine and CO_2. The related reactions are done considering harsh conditions like temperature higher than 200 °C, and a pressure higher than 6.0 MPa. For this reaction, only a few studies are reported in the case of heterogeneous catalysts. In the Ref. [10], polyethylene-glycol-supported potassium hydroxide is introduced as an efficient catalyst to synthesis cyclic urea from carbon dioxide and diamine, directly demonstrated a low yield of cyclic urea, under 80 bar pressure of carbon dioxide and at the temperature of 150 °C. This catalyst showed a low yield of product, at a pressure of 70 bar carbon dioxide and 140 °C. CeO_2 synthesized by biopolymer template method gave low yield for cyclic urea at 6 bar carbon dioxide pressure and 150 °C [11]. Tomishige et., al have proposed pure commercial CeO_2 as the most impressive catalyst among many different metal oxides like Al_2O, CaO, La_2O_3, TiO_2, MgO, Pr_6O_{11}, ZnO and ZrO_2. However, the catalyst of CeO_2 demonstrated appropriate catalytic activity in the case of CO_2 as well as amine reaction [10, 12–18].

Mesoporous silica materials can be used as a platform for many applications in diagnosis, therapeutics and pharmaceuticals [19]. SBA-15 as a mesoporous silica material, is widely utilized as supports in the case of heterogeneous catalysis due to the dispersity of active sites. In addition, for increasing the efficiency of mentioned materials, one can cofunctionalize them by other functional groups [20–22]. Moreover, SBA-15 can be utilized in wastewater purification, treatment and gas separation [23]. It is mesopore-rich and showed to have considerable internal surface area, high hydrothermal, plentiful surface hydroxyl groups and appropriate mechanical stability. Currently, in cases of catalyze reactions, a substantial number of catalysts like ionic liquids (ILs) [24, 25] as well as transition metal complexes [26, 27] were evaluated to be immobilized on SBA-15. Moreover, these immobilized catalysts demonstrated appropriate recyclability. SBA-15 is thought to be proper choice for stably-supporting multi-site ILs due to having mesoporous channel and plain loading [28–31].

Dendrimers are widely utilized in the field of catalysis because of their highly branched tridimensional structures and abundant peripheral groups as well as inimitable dendritic effects [32, 33]. Immobilization of dendrimer catalyst on support materials is an appearing area which attracted more consideration from chemists due to their simple and easy recoverability and reusability [34–36]. ILs as green chemistry compounds are utilized widely because of having promising attributes such as low flammability, low vapor pressure, good stability and so on. The adjustability of structure is known as the most significant characteristic of these compound. By the use of many functional groups in cations and anions having distinct structures, the physical and chemical attributes of ILs has been adjusted. Dendritic ILs (DILs) that have the properties of both dendrimers and ILs, were utilized in the fields of adsorption of heavy metal cations, transporters and catalysis [37, 38].

In this paper, many novel SBA-15 supported dendritic zwitterionic ionic liquid heterogeneous catalysts together with high-density active sites SBA-15/IL(1), SBA-15/IL(2), and SBA-15/IL(3) from SBA-15 (Scheme 1) are provided and after that are used as highly efficient and recyclable heterogeneous catalysts for synthesis of 2-imidazolidinone from CO_2 and ethylenediamine under mild conditions, as can be seen in Scheme 2. The high yields of appropriate 2-imidazolidinone can be achieved. The heterogeneous catalytic system is known to be reusable and stable for the synthesis of 2-imidazolidinone.

2 Experimental Section

2.1 General Approach for the Synthesis of SBA-15 NPs

SBA-15 is produced based on the Ref. [39]. TEOS is utilized as Pluronic (P123) and silica source is utilized as template. Firstly, 8.0 g of P123 and a constant amount of TEOS equal to 14.0 g are slowly added to an aqueous solution of HCl (3 mol/L, 180 ml) along with 70 g of water. For a day, whole considered mixtures is stirred under the temperature of 40 °C and after that was heated to the temperature of 120 °C for another 20 h considering static conditions. In the next step, the mesoporous material is filtered, washed by water up to when no $Cl-$ is not detected. The result compound is dried under the temperature of 45 °C considering vacuum condition. After that, the dried sample is dissolved in methanol and sonicated under the temperature of 45 °C for 15 min, then was filtered and repeated for four times. In the last step, the resulted compound is dried under vacuum under the temperature of 40 °C for obtaining SBA-15.

2.2 The Synthesis of Amino-Modified SBA-15 (SBA-15/APTS)

A small amount of SBA-15 equal to 5.0 g are released in 75 mL of NaOH solution (1.5 M). The obtained mixture is refluxed by applying the temperature of 150 °C at 1 h for improving its hydrophilicity. Then, the obtained fibers are washed for more than three times by water up to when the wash-water pH became neutral. Then, the activated fibers are dried in a vacuum oven and under 70 °C at 7 h and the activated luffa sponge fibers are functionalized by APTS for the preparation of amino-modified SBA-15/APTS. In detail,

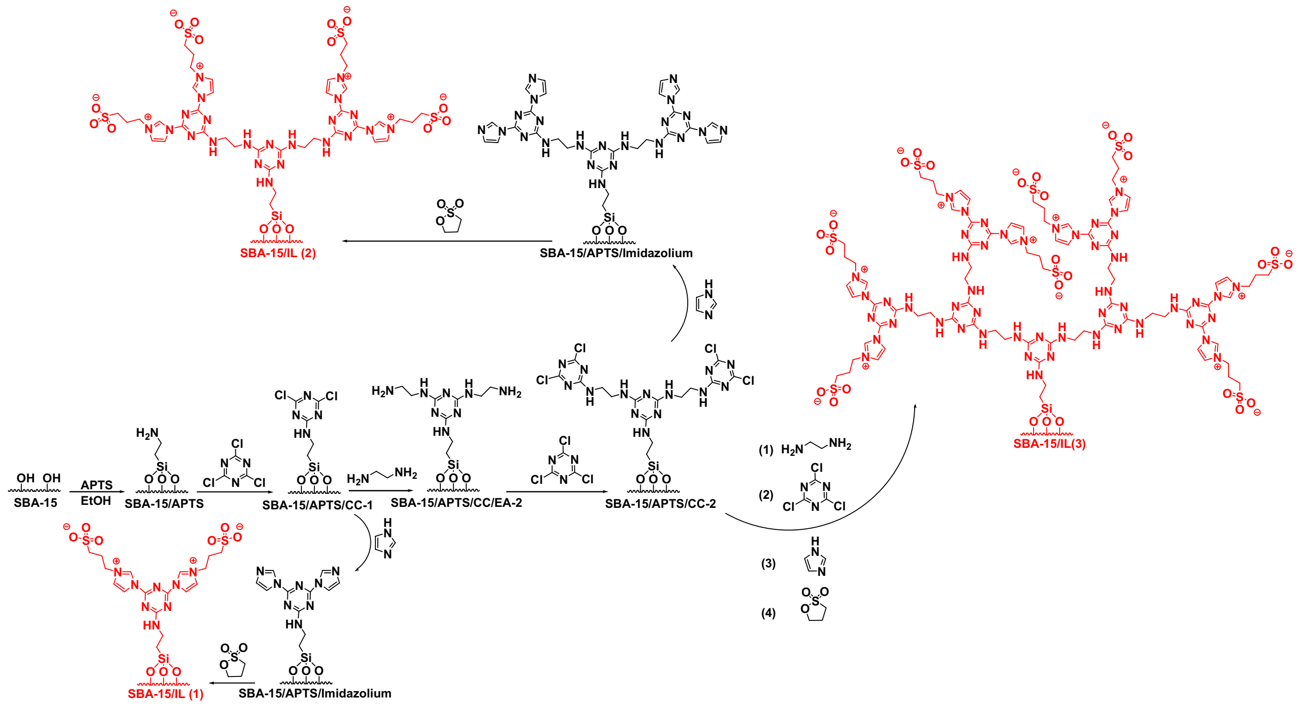

Scheme 1 Synthesis of the SBA-15/IL(1), SBA-15/IL(2), and SBA-15/IL(3)

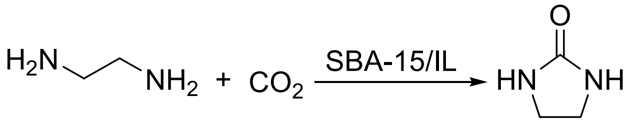

Scheme 2 Synthesis of 2-imidazolidinone from carbon dioxide and ethylenediamine in the presence of SBA-15/IL

4.0 g of activated luffa sponge fibers mixture and 7.0 mL of APTS, in 75 mL anhydrous ethanol is stirred under the temperature of 80 °C at a day, magnetically. After that, SBA-15/APTS is filtered and then washed by EtOH for three times and dried under the temperature of 60 °C at a half of day.

2.3 General Approach for the Synthesis of SBA-15/IL(1)

A mixture containing 2.6 mL of DIPEA, 3.1 g of cyanuric chloride (CC) and 3.2 g of SBA-15/APTS fibers is released in 40.0 mL of THF and is stirred under the temperature of 25 °C at a half of day. The metnioendmixture is filtered and the obtained fibers SBA-15/APTS/CC-1 are washed by using 5 mL × 6 of EtOAc and then dried at 10 h. 2.7 g of SBA-15/APTS/CC-1 is suspended in 55.0 mL of THF, 2.2 g of 1-imidazole are released, and the obtained mixture is stirred, magnetically, under 65 °C for a day. 100 mg of SBA-15/APTS/Imidazole is released in water: a mixture of ethanol (10:10 v/v, 100 mL) containing 2.5 g of 1,4-butanesultone. The reaction is performed under 25 °C for 2.0 h. The resulting mixture is then filtered, after that the filtrate is dried under vacuum under the temperature of 50 °C after the solvent is removed.

2.4 General Approach for the Synthesis of SBA-15/IL(2) and SBA-15/IL(3)

3.5 g of SBA-15/APTS/CC-1 in 60.0 mL of THF is released inethylenediamine DIPEA (8.41 mL). The mixture of reaction is stirred magnetically under the temperature of 85 °C at1 day. The obtained ethylenediamine-modified SBA-15/APTS/CC/EA-2 is filtered and then washed by using 5 mL × 6 of EtOAc and lastly dried in in vacuum oven under the temperature of 55 °C for 11 h. A mixture of 5.5 g of cyanuric chloride (CC) and ethylenediamine-modified 3.5 g of SBA-15/APTS/CC/EA-2 as well as 8.45 mL of diisopropylethylamine in 55 mL of THF is stirred under the temperature of 25 °C for 12 h, magnetically. After that, the filtration process in a proper way for separating the cyanuric chloride-modified fibers (SBA-15/APTS/CC-2). After each separation process SBA-15/APTS/CC-2 is washed by utilizing 5 mL × 6 of EtOAc and then dried in vacuo for a half of day. 3.5 g of SBA-15/APTS/CC-2 is suspended in THF (60 mL), 2.5 g of imidazole and 17.1 mL of DIPEA are released, and the mixture is magnetically stirred under the temperature of 90 °C at 1 day. The bio-based heterogeneous catalyst SBA-15/APTS/Imidazole (2) catalysis is washed by 5 mL × 6 of EtOAc and after that dried in in vacuum oven under the temperature of 50 °C for 12 h. SBA-15/APTS/Imidazole (3) can be produced utilizing the similar approach presented previously. A constant amount of SBA-15/APTS/Imidazole (2) or SBA-15/APTS/Imidazole (3) equal to 100 mg is released in water: a mixture of ethanol (10:10 v/v, 100 mL) containing 2.5 g of 1,4-butanesulton. The reaction is performed at 25 °C for 2.0 h. The obtained mixture is filtered, after which the filtrate is dried under vacuum under the temperature of 50 °C is the solvent was removed.

2.5 Representative Approach for the Synthesis of 2-imidazolidinone Catalysed by Utilizing SBA-15/IL Catalysts

Whole the cycloaddition reactions of carbon dioxide by ethylenediamine are performed in 20.0 mL of Teflon-lined stainless-steel reactor. In the reaction, a magnetic stirrer and a pressure gauge are attached. In the common approach, appropriate amount of ethylenediamine (10.0 mmol), SBA-15/IL catalyst, are added in the reactor. The reactor is purged three times by using carbon dioxide and the reactor is heated to an appropriate temperature and also pressure. The reactor is leaved in cold water. After that, the excess CO_2 is slowly released after occurring the reaction. 12 mL of EtOH is added in the mixture of reaction. Then, the catalyst of SBA-15/IL is recovered using filtration process. Lastly, the fabricated catalyst is washed two times by using methanol and dried under vacuum at room temperature.

3 Results and Discussion

Moreover, SEM and TEM analysis are used to characterize the morphology and also pore structure of the immobilized ILs (3) catalysts. Figure 1a and b shows the SEM images of immobilized ILs (3) catalysts. In addition, Fig. 1c and d shows the TEM images of immobilized ILs (3) catalysts. As seen, the strip sharp and regular appearance of SBA-15 and hexagonal structure of SBA-15 is clear, demonstrating the usual structure of SBA-15. Moreover, after loading ILs (3), the SBA-15 structure have not varied. As can be seen in Fig. 2, the decomposition conduct of the SBA-15 as well as dendritic ILs catalysts SBA-15/IL(1), SBA-15/

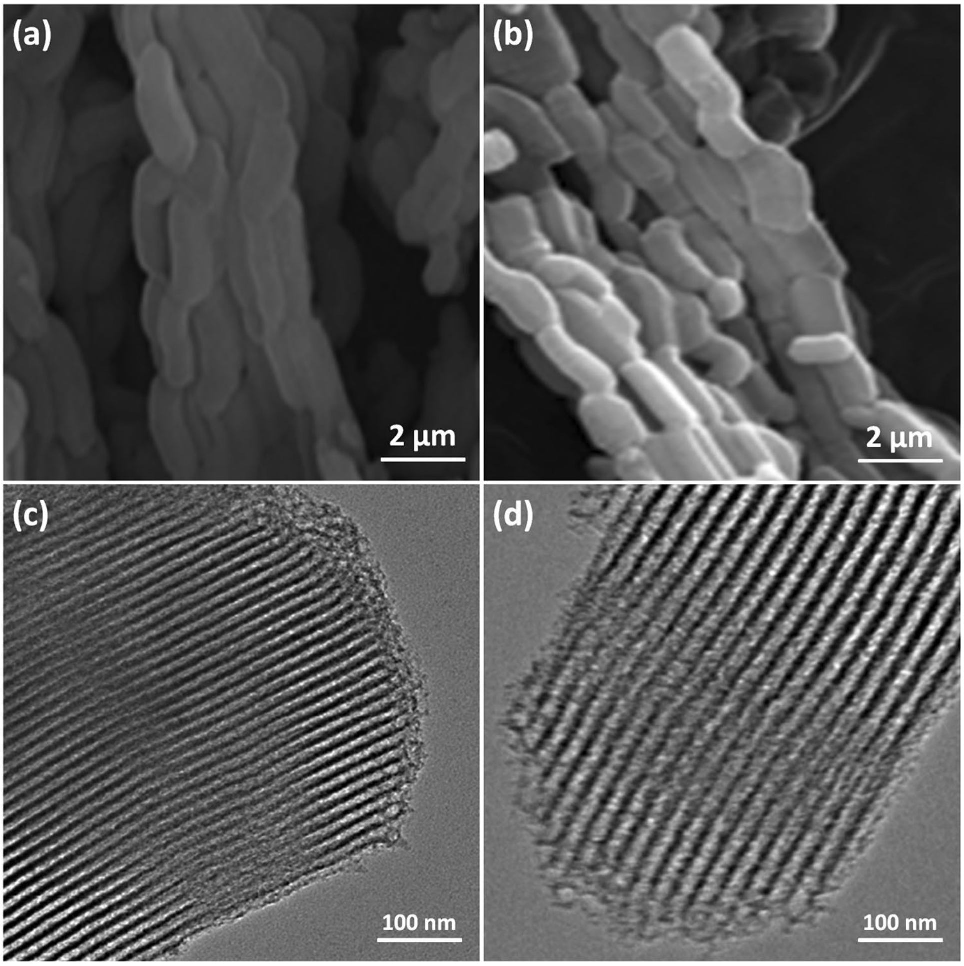

Fig. 1 SEM images of SBA-15 NPs (**a**); SBA-15 /IL(3) NPs (**b**); and TEM images of SBA-15 NPs (**c**); SBA-15/IL(3) NPs (**d**)

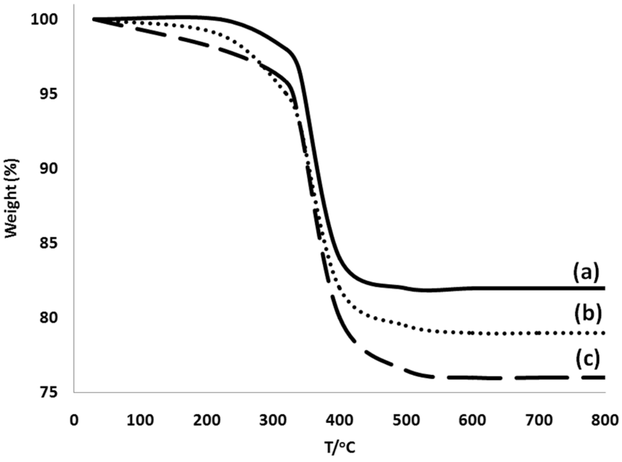

Fig. 2 TGA of *a* SBA-15/IL(1); *b* SBA-15/IL(2); and *c* SBA-15/IL(3)

IL(2) and SBA-15/IL(3) is compared for understanding the influences of the grafted dendritic IL molecules. In Fig. 2, the TGA analysis in the cases of SBA-15/IL(1), SBA-15/IL(2), and SBA-15/IL(3) are shown. As seen, all three mentioned samples demonstrated same thermal stability. As seen in the TGA curves, there are two processes of weight loss that the first process is determined among 25 °C and 100 °C demonstrated small weight loss equal to 5.0% related to the evaporation of physical adsorbed H_2O from the samples. Second one is between 300 °C and 450 °C demonstrated clear reduces by large weight loss of around 20–30% related to the lignin degradation.

Figure 3 shows the FT-IR spectroscopy pattern of the synthesized catalyst and its surface modification. As can be seen in Fig. 3a, for SBA-15, the bands at 1101 cm^{-1}, 798 cm^{-1}, and 1627 cm^{-1} demonstrated is related to Si–O–Si vibrations, the typical silanol group (Si–OH) stretching mode and the water absorbed onto the surface of solid, respectively. Many new appeared absorption peaks of 856 cm^{-1}, 1042 cm^{-1} and 1696 cm^{-1} in comparison with the FT-IR spectrum of luffa sponge (refer to Fig. 3a) is related to the stretching vibration of Si–O bond and the bending vibrations of C = N bond on the surface of SBA-15/IL, respectively. In addition to the mentioned peaks, the broad peak at 1044 cm^{-1} is related to S = O stretching vibrations in the sulphonate functional groups. Bands at 1493 cm^{-1} are belonged to N–H bending vibrations in the ammonium groups. It was demonstrated that IL is immobilized onto SBA-15 NPs, successfully.

The N_2 adsorption–desorption isotherms of SBA-15, SBA-15/IL(1), SBA-15/IL(2), and SBA-15/IL(3) showed a distinct type IV curve, which was consistent with past

Fig. 3 FTIR spectra of SBA-15 (*a*); and SBA-15/IL (*b*)

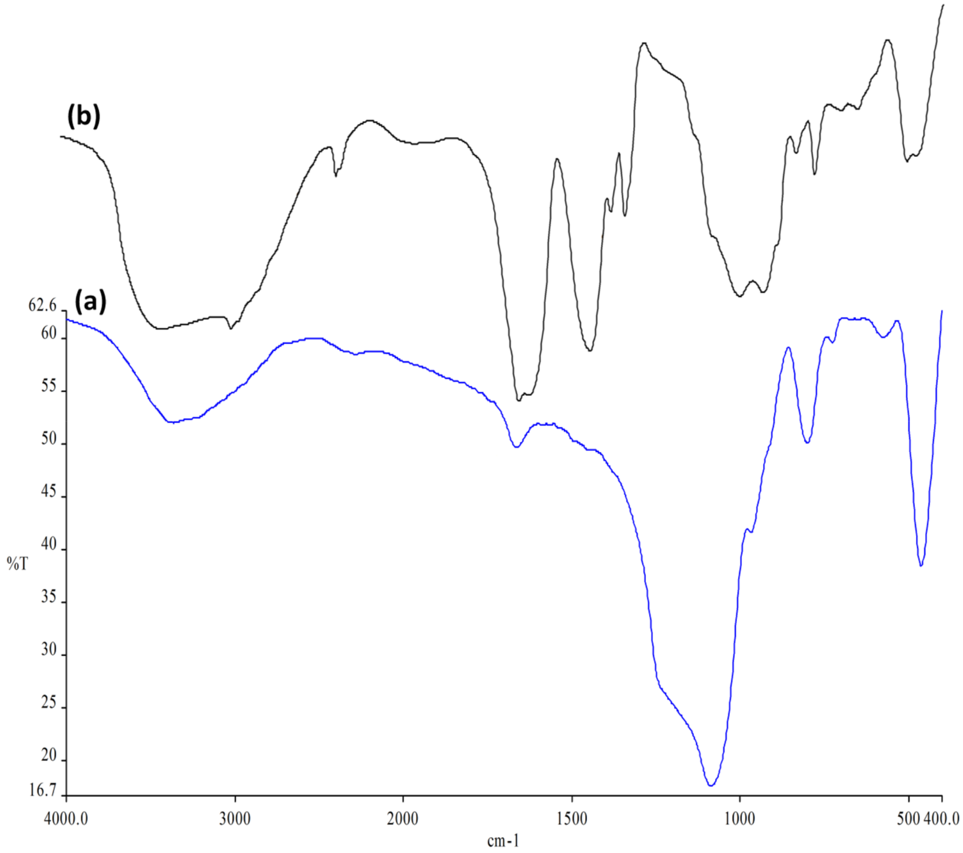

researches on standard fibrous silica spheres (Fig. 4). Table 1 illustrates that the produced SBA-15 possessed similar properties as commercial the SBA-15 and SBA-15, before and after grafting demonstrates a considerable large difference. In cases of SBA-15/IL(1), SBA-15/IL(2), and SBA-15/IL(3), the surface areas of BET are determined to be 331 m^2g^{-1}, 302 m^2g^{-1}, and 254 m^2g^{-1}; pore diameters are equal to 6.58 nm, 6.55 nm, and 6.51 nm; and pore volumes 0.55 cm^3g^{-1}, 0.52 cm^3g^{-1}, and 0.41 cm^3g^{-1}, respectively. Compared to pristine SBA-15, the SBA-15/IL nitrogen sorption analysis has demonstrated a regular and uniform mesostructure having a reduction of surface area, pore diameter and pore volume parameters. The related pore volumes were considerably decreased by the functionalization using X-Si (X = IL(1), IL(2), and IL(3)). As seen, ILs are immobilized onto SBA-15 that is related to reducing surface area as well as total pore volume, (refer to Table 1). The BET surface area, pore diameter, and total pore volume of BJH of the used catalyst were compared with those of the fresh catalyst. It was found that the anatomy of the used catalyst remained undamaged after three recycles.

The catalytic activity of the different kinds of dendritic imidazolium ILs catalysts (i.e., SBA-15/IL(1), SBA-15/IL(2), and SBA-15/IL(3)) are examined by synthesis of 2-imidazolidinone from carbon dioxide and ethylenediamine (refer to Table 2). The reaction performed deploying SBA-15 showed that no amount of the 2-imidazolidinone was formed (Table 2, row 2). Product yields equal to 76–94% are achieved utilizing the 25 mg of SBA-15/IL(1), SBA-15/IL(2), or SBA-15/IL(3) as catalysis after 10 h. It is found that, by the increase in the generation of the dendritic ILs, the catalytic activity enhanced. To improve the reaction situations, the synthesis of 2-imidazolidinone in the presence of SBA-15/IL(3) was selected.

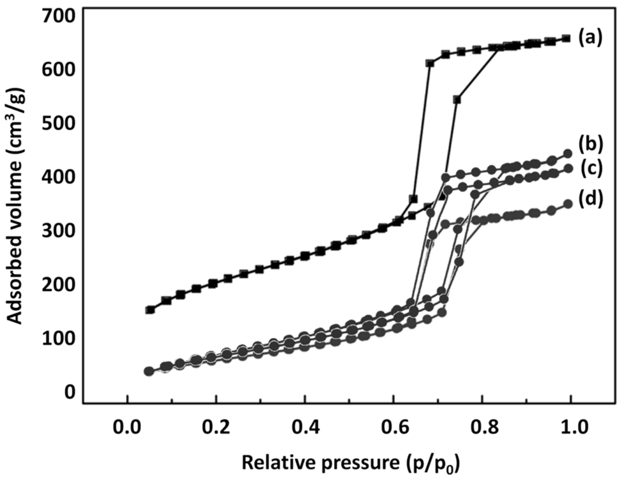

Fig. 4 Adsorption–desorption isotherms of *a* SBA-15, *b* SBA-15/IL(1), *c* SBA-15/IL(2), and *d* SBA-15/IL(3)

Table 1 Structural parameters of SBA-15, SBA-15/IL(1), SBA-15/IL(2), and SBA-15/IL(3) materials determined from nitrogen sorption experiments

Catalysts	S_{BET} (m^2 g^{-1})	V_t (cm^3 g^{-1})	D_{BJH} (nm)
SBA-15	536	0.97	6.67
SBA-15/IL(1)	331	0.55	6.58
SBA-15/IL(2)	302	0.52	6.55
SBA-15/IL(3)	254	0.41	6.51
SBA-15/IL(3) after three reuses	261	0.43	6.64

The catalytic activity of the SBA-15/IL(3) NPs are examined by synthesis of 2-imidazolidinone from carbon dioxide and ethylenediamine (refer to Table 3). Moderate to good to excellent yields were obtained under different solvent conditions (refer to Table 3). We have demonstrated that the solvent-free condition caused to obtaining better results compared to using organic solvents by taking into consideration of the yield of the synthesis of 2-imidazolidinone.

After wards, in the cases of subsequent reactions, we investigated the SBA-15/IL(3) catalyst for obtaining the optimized reaction conditions. The effect of temperature, reaction time and CO_2 pressure as well as amount of SBA-15/IL(3) catalyst on the reaction of cycloaddition is evaluated. As seen in Fig. 5, the temperature of reaction possessed a dramatic effect on the 2-imidazolidinone yield. The 2-imidazolidinone yield can enhance by the enhancement of reaction temperature ranging from 30 °C to 70 °C (94%, 70 °C) and levels off upon more enhancing temperature equal to 100 °C.

Table 4 shows that the enhancement of the catalyst amount from 5 mg to 10 mg, 15 mg, 20 mg, and 25 mg can enhance the yield of cycloaddition from 22 to 53, 71, 94, and 94, respectively. It is clear that, the 2-imidazolidinone by the enhancement of catalyst amount. With using 20 mg of SBA-15/IL(3), a yield about 94% is achieved. Noted that, more enhancement of catalyst amount cannot change the 2-imidazolidinone yield considerably. Figures 6 demonstrate the effect of reaction time at the presence of CO_2 under the temperature of 70 °C and 1.5 bar. The 2-imidazolidinone yield

Table 2 Synthesis of 2-imidazolidinone by different of SBA-15/IL NPs

Entry	Catalyst	Yield (%)[a]
1	None	-
2	SBA-15	-
3	SBA-15/IL(1)	76
4	SBA-15/IL(2)	85
5	SBA-15/IL(3)	94

[a] Isolated yields

Table 3 Synthesis of 2-imidazolidinone from carbon dioxide and ethylenediamine by SBA-15/IL(3) in different solvents[a]

Entry	Solvent	Yield (%)[b]
1	Solvent-free	94
2	DMF	31
3	DMSO	44
4	Dioxane	52
5	CH_3CN	40
6	EtOAc	56
7	THF	38
8	Toluene	41
9	CH_2Cl_2	56
10	$CHCl_3$	42
11	CCl_4	8
12	n-Hexane	10
13	Benzene	13
14	Cyclohexane	19
15	H_2O	72
16	EtOH	64
17	i-PrOH	41
18	MeOH	52

[a] Reaction conditions: ethylenediamine (5.0 mmol), CO_2 (2.5 Mpa) and SBA-15/IL(3) (20 mg) at 100 °C for 12 h

[b] Isolated yields

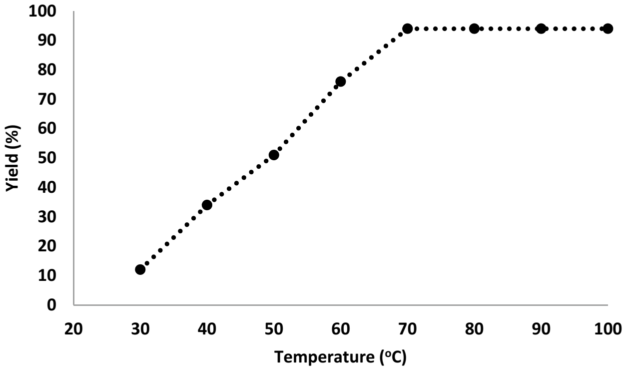

Fig. 5 Effect of temperature on yield of synthesis of 2-imidazolidinone. Reaction conditions: ethylenediamine (5.0 mmol), CO_2 (2.5 Mpa) and SBA-15/IL(3) (20 mg) for 12 h

Table 4 Effect of amount of catalyst on yield of synthesis of 2-imidazolidinone[a]

Entry	Amount of SBA-15/IL (mg)	Yield (%)	TON
1	5	22	36.6
2	10	53	88.3
3	15	71	118.3
4	20	94	156.6
5	25	94	156.6

[a] Reaction conditions: ethylenediamine (5.0 mmol), and CO_2 (2.5 Mpa) at 70 °C for 12 h

[b] Isolated yields

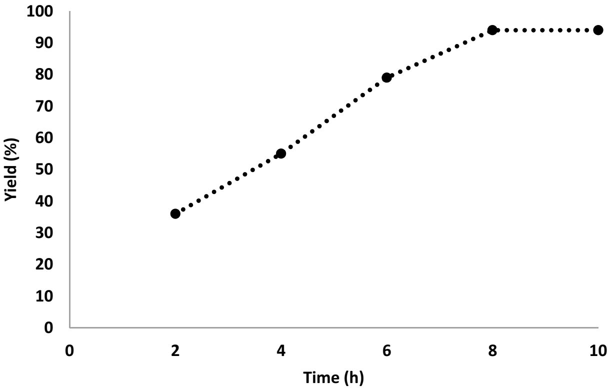

Fig. 6 Effect of time on yield of synthesis of 2-imidazolidinone. Reaction conditions: ethylenediamine (5.0 mmol), CO_2 (2.5 Mpa) and SBA-15/IL(3) (20 mg) at 70 °C

possessed a gradual enhancing from 2 h to 8 h (94%, 8 h). After that, remaining unvaried in all time approximately. It is obvious that ethylenediamine is almost converted in the target product only in 8 h.

Moreover, the pressure of CO_2 is investigated to increase the production of 2-imidazolidinone. The promised CO_2 pressure to obtain the most appropriate preparation of SBA-15/IL(3) NPs can be determined in the meantime the kinetics related to the mass transfer reactions can be varied by taking into considerations of both diffusion and the reaction of CO_2 to ethylenediamine. The effect of pressure is specified, experimentally, in the range of 0.5 MPa to 2.5 MPa pressure. The SBA-15/IL(3) NPs function forcefully enhanced when the pressure of CO_2 increased from 0.5 MPa to 1.5 MPa pressure. Then, it is supportable for the pressure in the range of 1.5 MPa to 2.5 MPa demonstrated in Fig. 7. These outcomes demonstrated the requirement considering an optimum pressure about the pressure of 1.5 bar for the desired products of 2-imidazolidinone. Also, the effects of concentration of ethylenediamine was investigated. The reaction order with respect to ethylenediamine concentration was almost zero, which indicates that the diamine is strongly adsorbed on catalyst. [12, 40]

Product syntheses from CO_2, and diamines were examined comprehensively (Table 5). 1,2-propanediamine, 2-methyl-1,2-propanediamine, and ethylenediamine (Table 5, entries 1–3) reacted to afford the corresponding cyclic ureas in excellent yields (92–95%). *N*-Alkyl ethylenediamines (Table 5, entry 4) were also converted selectively. However, *N*,*N′*-dimethylethylenediamine was converted in good yield (89%) (Table 5, entry 5). The amplitude of substrate scope was investigated with different aminoalcohols over SBA-15/

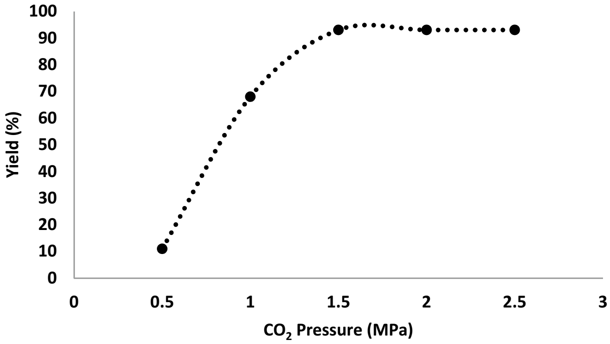

Fig. 7 The effect of carbon dioxide pressure on the synthesis of 2-imidazolidinone. Reaction conditions: ethylenediamine (5.0 mmol), and SBA-15/IL(3) (20 mg) at 70 °C for 8 h

IL(3), the results of which are illustrated in Table 5. Aminoethanols (Table 5, rows 6–8) were quantitatively converted to the corresponding five-membered-ring cyclic carbamates at high efficiencies [41, 42]. The use of o-phenylenediamines with electron receptor groups was resulted in good efficiencies due to a decrease of the electron density of the nitrogen atom (Table 5, rows 9–11). On the other hand, only a trace of aniline was observed, which might be due to the fact that CO_2 reactions with these substrates are equilibrium restricted. Aniline reacted with difficulty (Table 5, entry 12), which was due to the low nucleophilicity of aniline [11].

For a deeper evaluation of the efficiency of the catalyst, various control experiments were conducted (Table 6). The reaction performed deploying SBA-15 showed that no amount of the 2-imidazolidinone was formed after 12 h (Table 6, row 1). Also, no reaction was perceived when SBA-15/APTS was employed as a catalyst (Table 6, row 2). APTS is not able to show catalytic activity. Due to these unfavorable results, we continued research to increase efficiency by adding ionic liquid (Table 6, row 3). Our results show that the reaction is primarily catalyzed using ionic liquid in the SBA-15/APTS nanostructure. Nanoparticles increase the activity of the catalyst due to the increase in surface area to volume, so they significantly increase the sensitivity between the reactants and the catalyst and act as a homogeneous catalyst (Table 6, rows 3 and 4). In addition, the activity and selectivity of nano-catalysts can be controlled by adjusting the chemical and physical characteristics such as size, form, composition, and morphology. To evaluate the real influence of the existence of SBA-15 in the catalyst, the SBA-15/IL(3) NPs were compared with MCM-41/IL(3) and nano-SiO_2/IL(3) (Table 6, rows 5 and 6). The use of MCM-41/IL(3) and nano-SiO_2/IL(3) as the catalyst led to a good efficiency of the desired product; however, the efficiency for SBA-15/IL(3) was superb. The tangible activity of the silica was assigned to its form, composition, and morphology. Furthermore, the large space between the pores can remarkably enhance the availability of the active sites of the SBA-15. For this reason, the SBA-15 was more efficient than MCM-41 and nano-SiO_2 (Table 6, rows 3 and 5).

Table 7 presents information about catalysts and reagents for the direct reaction of diamines with carbon dioxide [43]. As mentioned in the section on cyclic carbamates synthesis, the reaction system consisting of the DPPA and PhTMG was efficient for the synthesis of 2-imidazolidinone (Table 7, row 1). $TBA_2[WO_4]$ and Ph_3SbO/P_4S_{10} were introduced as catalysts (Table 7, rows 2 and 3). The reaction by Ph_3SbO/P_4S_{10} continued in the same reaction pathway mentioned in the synthesis of carbamate by catalysts. The $TBA_2[WO_4]$ introduced by Mizuno was an effective homogeneous substance for the synthesis of 2-imidazolidinone from atmospheric carbon dioxide and diamines. The activity of the $TBA_2[WO_4]$ catalyst was done by the activation of carbon dioxide by the weak Lewis basic feature and the absorption of diamineby-hydrogen bonding [4, 5]. CeO_2 and KOH/PEG1000 were reported as catalysts (Table 7, rows 4 and 5) [8, 40]. CeO_2 NPs synthesized by biopolymer template techniques and the employment of mesoporous alginate aerogel was an effective catalyst at 433 K and 0.7 MPa carbon dioxide pressure. This catalyst suffered from disadvantages such as a narrow bed of substrates and low product efficiencies. In contrast, it has recently been shown that pure CeO_2 acted as an efficient heterogeneous catalyst in isopropyl alcohol (IPA) solvent, even at a low carbon dioxide pressure of 0.3 MPa, to provide high-yield cyclic urea [12].

In green chemistry, the catalyst reusability state is considered a significant property. Therefore, the reuse of the SBA-15/IL(3) NPs was investigated with respect to the optimal state of synthesis of 2-imidazolidinone. SBA-15/IL(3) NPs were easily isolated from the liquid reaction zone after a few seconds. The solvent can be used quickly after cleaning. As Fig. 8 illustrates, the catalyst was recycled for ten consecutive cycles. Product yield in the tenth run was 89%, showing merely a 5% decrease in performance compared to the fresh catalyst.

Finally, we carried out a leaching experiment to explore the homogeneity of the catalyst system. This reaction was initially done deploying optimized circumstances, in the participation of the ten-times recycled catalyst. After 4 h of reaction, the catalyst was separated by hot filtration and the solution was mixed for 4 h. Figure 9 illustrates the synthesis of 2-imidazolidinone as a function of time with the ten-times recycled catalyst (black curve). As Fig. 10 shows, the employment of the reagent was no longer observed after the isolation of the catalyst (red curve).

The obtained analyzes of SEM and TEM demonstrated the more data in the case of the fibrous NPs of SBA-15/IL(3). In the case of new fibrous NPs of SBA-15/IL(3), the analyzes of SEM and TEM for, and the 10th fibrous NPs SBA-15/IL(3) reused were determined as shown in Fig. 10a and b,

Table 5 Scope of diamines for synthesis of the cyclic urea[a]

Entry	Diamine	Cyclic urea	Conversion (%)	Yield (%)[b]	
				Cyclic urea	*N*-Alkylated amine
1	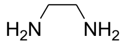	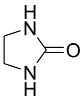	98	94	Trace
2	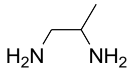	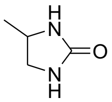	98	95	Trace
3	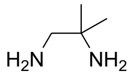	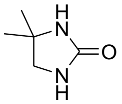	97	92	2
4	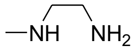	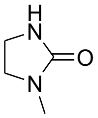	98	90	Trace
5	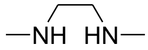	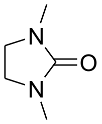	96	89	4
6	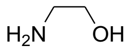	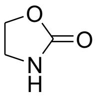	94	96	2
7	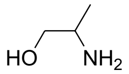	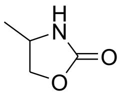	97	95	3
8	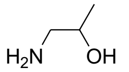	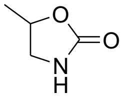	97	96	Trace
9	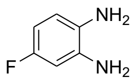	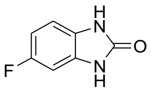	99	92	Trace
10	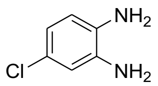	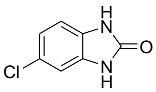	97	95	1
11	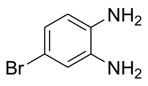	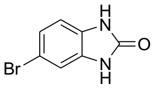	98	93	Trace
12	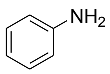	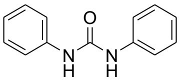	Trace	Trace	Trace

[a] Reaction conditions: ethylenediamine (5.0 mmol), CO_2 (1.5 Mpa) and SBA-15/IL(3) (20 mg) at 70 °C for 8 h

[b] Isolated yields

respectively. After being 10th reusing of the catalyst, the tube-like structure of the catalyst is still obvious. The desired power in recyclability is specified because of existing the identical structure of fresh fibrous NPs of SBA-15/IL(3) and SBA-15/IL(3) 10th reused. Moreover, after 10 runs recycling, the thermal stability of mentioned catalysis is not appropriate as the

Table 6 Influence of different catalysts for the synthesis of 2-imidazolidinone[a]

Entry	Catalyst	Yield (%)[b]
1	SBA-15	–
2	SBA-15/APTS	–
3	SBA-15/IL(3)	94
4	IL(3)	95
5	MCM-41/IL(3)	88
6	nano-SiO_2/IL(3)	72

[a] Reaction conditions: ethylenediamine (5.0 mmol), CO_2 (1.5 Mpa) at 70 °C for 12 h

[b] Isolated yield

Table 7 2-imidazolidinone syntheses from diamine and carbon dioxide

Entry	Catalyst	Yield (%)	References
1	DPPA/ PhTMG	86	[43]
2	$TBA_2[WO_4]$	91	[4]
3	Ph_3SbO/P_4S_{10}	85	[5]
4	KOH/PEG1000	82	[8]
5	CeO_2	96	[40]
6	SBA-15/IL(3)	94	This work

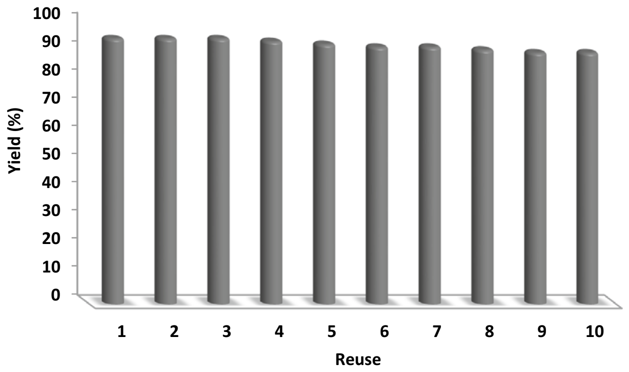

Fig. 8 Recyclability of the catalyst. Reaction conditions: ethylenediamine (5.0 mmol), CO_2 (1.5 Mpa) and SBA-15/IL(3) (20 mg) at 70 °C for 8 h

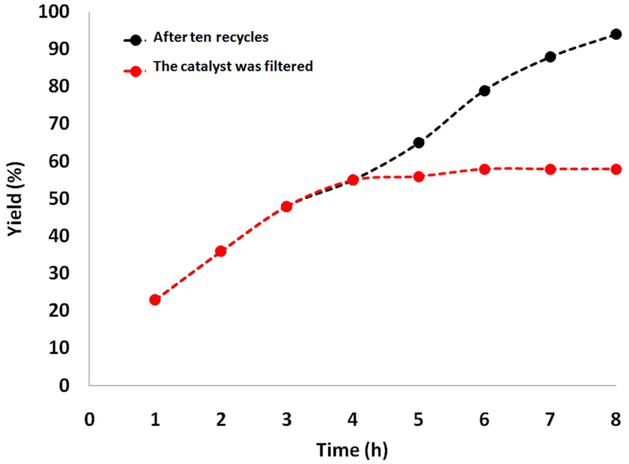

Fig. 9 Leaching test for the catalyst of the synthesis of 2-imidazolidinone

fresh catalyst casued by the loss of IL in SBA-15 fibers in the process of recycling (reffer to Fig. 11). However, it has not affect its practicability while utilized under the temperature of 100 °C.

4 Conclusions

In this study, the synthesis of SBA-15 supported dendritic ILs catalysts SBA-15/IL(1), SBA-15/IL(2), and SBA-15/IL(3) possessing high ionic density and distinct generations are reported for the first time. We observed that there exists a positive dendritic impact of the dendritic ILs catalysts SBA-15/IL(1), SBA-15/IL(2), and SBA-15/IL(3) onto the product yield of the synthesis of 2-imidazolidinone from carbon dioxide and ethylenediamine. Between the introduced catalysts, SBA-15/IL(3) showed to have the optimal heterogeneous catalytic conduct and have appropriate catalytic activity in the case of the synthesis of 2-imidazolidinones, providing excellent yields. SBA-15/IL(3) can be recycled until 10 consecutive runs without any dramatic reduction in catalytic activity. SBA-15/IL(3) demonstrated many promising benefits than the reported heterogeneous catalysts, like low cost, easy preparation and higher catalytic potential as well as renewable nature in the case of the synthesis of 2-imidazolidinones that introduced it a proper candidate for different practical usages.

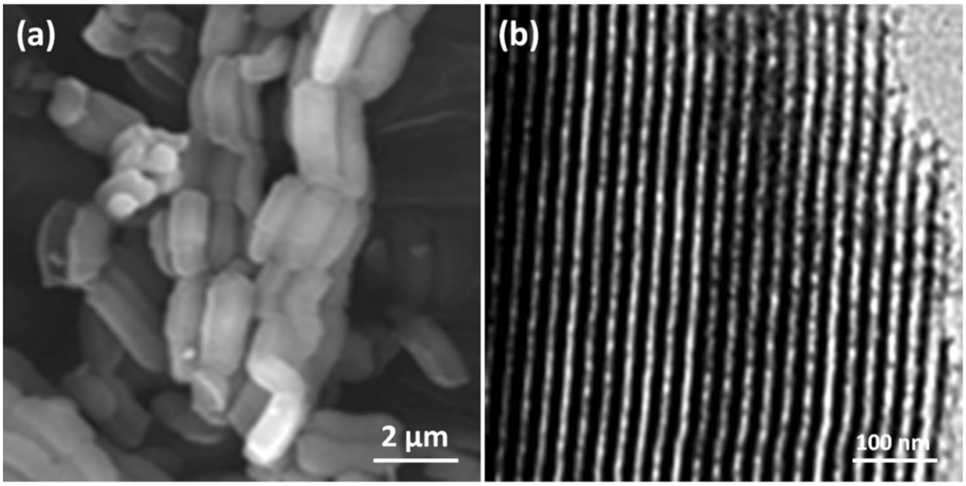

Fig. 10 **a** FE-SEM, and **b** TEM images of the recovered SBA-15/IL(3) NPs after the 10 th run for the synthesis of 2-imidazolidinone

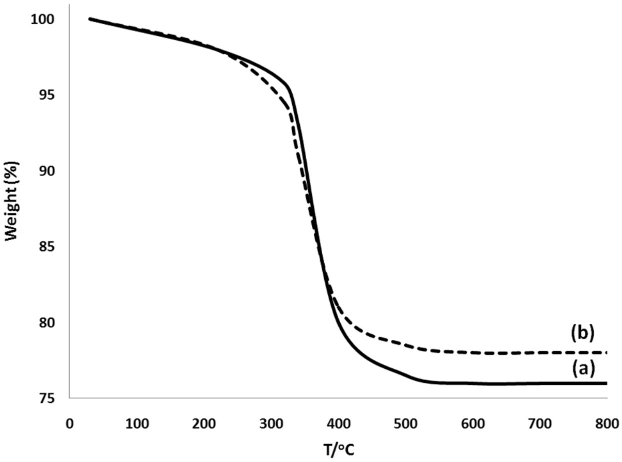

Fig. 11 TGA of the fresh SBA-15/IL(3) catalyst (**a**) and the reused SBA-15/IL(3) catalyst after 10 times recycling (**b**)

Acknowledgements This work was sponsored in part by Natural Science Foundation of Liaoning Province (No. 20170520296)

References

1. Kondo K, Yokoyama S, Miyoshi N, Murai S, Sonoda N (1979) Angew Chem 18:691–691
2. Flosi WJ, DeGoey DA, Grampovnik DJ, Chen H-J, Klein LL, Dekhtyar T (2006) Bioorg Med Chem 14:6695–6712
3. Leung M-k, Lai J-L, Lau K-H, Yu H-h, Hsiao H-J (1996) J Org Chem 61:4175–4179
4. Nomura R, Hasegawa Y, Ishimoto M, Toyosaki T, Matsuda H (1992) J Org Chem 57:7339–7342
5. Kimura T, Kamata K, Mizuno N (2012) Angew Chem 51:6700–6703
6. Bhanage BM, Fujita S-I, Ikushima Y, Arai M (2003) Green Chem. 5:340–342
7. Wu C, Cheng H, Liu R, Wang Q, Hao Y, Yu Y, Zhao F (2010) Green Chem 12:1811–1816
8. Kong D-L, He L-N, Wang J-Q (2010) Synlett 2010:1276–1280
9. Primo A, Aguado E, Garcia H (2013) ChemCatChem 5:1020–1023
10. Hwang J, Han D, Oh JJ, Cheong M, Koo H-J, Lee JS, Kim HS (2019) Adv Synth Catal 361:297–306
11. Tomishige K, Tamura M, Nakagawa Y (2019) Chem Rec 19:1354–1379
12. Tamura M, Honda M, Nakagawa Y, Tomishige K (2014) J Chem Technol Biotechnol 89:19–33
13. Honda M, Sonehara S, Yasuda H, Nakagawa Y, Tomishige K (2011) Green Chem 13:3406–3413
14. Truong CC, Mishra DK (2020). Environ Chem Lett. https://doi.org/10.1007/s10311-020-01121-7
15. Tamura M, Miura A, Honda M, Gu Y, Nakagawa Y, Tomishige K (2018) ChemCatChem 10:4821–4825
16. Gu Y, Miura A, Tamura M, Nakagawa Y, Tomishige K (2019) ACS Sustainable Chem Eng 7:16795–16802
17. Kulal N, John C, Shanbhag GV (2020) Appl. Catal. A 598:117550
18. Alferov KA, Fu Z, Ye S, Han D, Wang S, Xiao M, Meng Y (2019) ACS Sustain Chem Eng 7:10708–10715
19. Popat A, Hartono SB, Stahr F, Liu J, Qiao SZ, Lu GQ (2011) Nanoscale 3:2801–2818
20. Doustkhah E, Rostamnia S, Hassankhani A (2016) J Porous Mater 23:549–556
21. Doustkhah E, Rostamnia S (2016) Mater Chem Phys 177:229–235
22. Doustkhah E, Lin J, Rostamnia S, Len C, Luque R, Luo X, Bando Y, Wu KCW, Kim J, Yamauchi Y, Ide Y (2019) Chem Eur J 25:1614–1635
23. Ji G, Zhang Y, Shen J (2015) Nat Gas Chem Indust 40:84–88
24. Rostamnia S, Golchin Hossieni H, Doustkhah E (2015) J Organomet Chem 791:18–23
25. Rostamnia S, Doustkhah E, Bulgar R, Zeynizadeh B (2016) Microporous Mesoporous Mater 225:272–279
26. Hosseini HG, Doustkhah E, Kirillova MV, Rostamnia S, Mahmoudi G, Kirillov AM (2017) Appl Catal A Gen 548:96–102
27. Rostamnia S, Doustkhah E, Zeynizadeh B (2016) Microporous Mesoporous Mater 222:87–93
28. Kruk M, Jaroniec M, Ko CH, Ryoo R (2000) Chem Mater 12:1961–1968
29. Yue MB, Chun Y, Cao Y, Dong X, Zhu JH (2006) Adv Funct Mater 16:1717–1722
30. Karimi B, Vafaeezadeh M (2012) Chem Commun 48:3327–3329
31. Zhong S, Liang L, Liu M, Liu B, Sun J (2015) J. CO_2 Util. 9:58–65.

32. Astruc D, Boisselier E, Ornelas C (2010) Chem Rev 110:1857–1959
33. Tomalia DA (2012) New J Chem 36:264–281
34. Giacalone F, Campisciano V, Calabrese C, Parola VL, Syrgiannis Z (2016) Prato M 10:4627–4636
35. Sadjadi S, Malmir M, Heravi MM (2019) Appl Clay Sci 168:184–195
36. Murugan E, Jebaranjitham JN, Raman KJ, Mandal A, Geethalakshmi D, Kumarc MD, Saravanakumarc A (2017) New J Chem 41:10860–10871
37. Qin TY, Li XY, Chen JP, Zeng Y, Yu TJ, Yang GQ, Li Y (2014) Chem Asian J 9:3641–3649
38. Hayouni S, Robert A, Maes C, Conreux A, Marin B, Mohamadou A (2018) New J Chem 42:18010–18020
39. Shi Z, Su Q, Ying T, Tan X, Deng L, Dong L, Cheng W (2020) J. CO_2 Util. 39:101162.
40. Tamura M, Noro K, Honda M, Nakagawa Y, Tomishige K (2013) Green Chem 15:1567–1577
41. Tamura M, Ito K, Nakagawa Y, Tomishige K (2016) J Catal 343:75–85
42. Tamura M, Honda M, Noro K, Nakagawa Y, Tomishige K (2013) J Catal 305:191–203
43. Paz J, Perez-Balado C, Iglesias B, Munoz L (2010) J Org Chem 75:3037–3046